Received February 28, 2020, accepted March 20, 2020, date of publication March 24, 2020, date of current version April 8, 2020.

Digital Object Identifier 10.1109/ACCESS.2020.2982999

A Precise-Integration Time-Domain Formulation Based on Auxiliary Differential Equation for Transient Propagation in Plasma

ZHEN KANG[1], (Member, IEEE), WEILIN LI[1], (Member, IEEE), YUFENG WANG[1], MING HUANG[1], AND FANG YANG[2]

[1]Department of Electrical Engineering, School of Automation, Northwestern Polytechnical University, Xi'an 710072, China
[2]School of Electrical and Control Engineering, Xi'an University of Science and Technology, Xi'an 710054, China

Corresponding author: Ming Huang (minghuang@nwpu.edu.cn)

This work was supported by the China Postdoctoral Science Foundation under Grant 2019M653737, and in part by the National Natural Science Foundation of Shaanxi Province under Grant 2019JQ-226.

ABSTRACT The electromagnetic wave propagation through plasma medium is one of the most important research fields in computational electromagnetics. A numerical formulation based on both the auxiliary differential equation (ADE) and the precise-integration time-domain (PITD) method for solving the plasma problems is proposed to break through the Courant-Friedrich-Levy (CFL) limit on the time-step size in a finite-difference time-domain (FDTD) simulation. In this new method, the current density J is introduced as the auxiliary variable to deal with the complex permittivity of the plasma which is dependent on the frequency, and the precise integration (PI) technique makes the selectable maximum time-step size become much larger and removes the impact of the time-step size to the numerical dispersion error. Numerical experimentations of the typical plasma problems verify and validate the reliability of the proposed formulation. Through the numerical results, it can be found that the maximum allowable time-step size of the new method is much larger than that of the CFL limit of the FDTD method, and the calculation error of the new method is nearly independent of the time-step size. As a consequence, the execution time is significantly reduced by using a larger time-step size.

INDEX TERMS Auxiliary differential equation, computational electromagnetics, numerical solution, plasma, precise-integration time-domain (PITD) method.

I. INTRODUCTION

Calculation of the electromagnetic wave propagation through dispersive materials, e.g., plasma, is a complex problem and has attracted much attention in recent years [1]–[3]. The simulation of these complex media can be applied in various areas of interest to the electromagnetic compatibility (EMC) society, such as the complex printed boards (PCSs) design [4], [5], the analysis of the absorption characteristics [6], [7], the simulations of metamaterials [8]–[10], the FDTD chamber model [11] and so on. The most popular methods for plasma even other dispersion materials are the algorithms based on the finite-difference time-domain (FDTD) method. The most frequently used FDTD methods can be categorized into three types: the recursive convolution (RC) method [12]–[14], the auxiliary differential equation (ADE) method [15]–[17], and the Z-transform (ZT) method [18]–[21]. These algorithms based on the FDTD method have two significant problems, the limit of the Courant-Friedrich-Levy (CFL) condition and the increasing numerical dispersion error, which have limited the intense utilization of the FDTD method as the problem size expands. If the mesh density is very fine, the time-step size becomes extremely small because of the CFL limit so that it results in exceedingly high computational memory requirement.

In attempt to improve the efficiency of the popular FDTD method, Namiki, Zheng, et al propose the alternating-direction implicit FDTD (ADI-FDTD) method which is an unconditionally stable time-domain algorithm for solving Maxwell's equations [22]–[25]. The ADI-FDTD method known as the implicit finite-difference algorithm without the limit of the CFL condition improves the computational

The associate editor coordinating the review of this manuscript and approving it for publication was Muhammad Zubair.

efficiency by using larger time-step size. Recently, some researchers have generalized the ADI-FDTD method to the application of the dispersion materials [26], [27]. However, the time-step size of the ADI-FDTD method cannot be selected too large, because of the contradiction between the time-step size and the numerical dispersion error. If the time-step size increases, the numerical dispersion error will be rapidly deteriorative. In addition, the locally-one-dimensional (LOD) FDTD method is also an unconditional stable algorithm [28], [29], and it has been widely used to solve the dispersion problems based on ADE technique [30]–[32]. Compared with the ADI-FDTD method, the LOD-FDTD method has better computational efficiency because of the fewer arithmetic operations required in the LOD algorithm. Nevertheless, both methods provide the comparable accuracy.

In recent years, a new 3-D time-domain method, called precise-integration time-domain (PITD) method, has attracted much attention for solving Maxwell's equations in free space and lossy space [33]–[38], since the PITD method breaks through the limit of the CFL condition on the time-step size in a FDTD simulation. The basic idea of the PITD method is approximating the spatial derivative with the central finite-difference scheme and reducing Maxwell's curl equations to a set of ordinary differential equations (ODEs), and then solving the ODEs by using the precise-integration (PI) technique [39]. Compared with the FDTD method, the most significant advantage of the PITD method is using a time-step size which is much larger than that of the CFL stability condition. Furthermore, the numerical dispersion errors can be made nearly independent of the time-step size. In contrast to the ADI-FDTD method, the selection of the time-step size has no effect to the computational accuracy in the PITD method. The numerical dispersion error of the PITD method is also smaller than that of the conventional ADI-FDTD method.

In this paper, prompted by the above-mentioned reasons, we consider using the PITD method to solve the electromagnetic problems in plasma. By introducing the polarization current density as the auxiliary variable, Maxwell's equations in plasma medium are obtained. The accuracy and efficiency of this new proposed algorithm are verified by modeling electromagnetic wave propagation through the infinite plasma space, the plasma slab, the plasma photonic crystal and 2-D cavity. Furthermore, the numerical experimentations also validate that the PITD method in plasma still keep its characteristics in free space and lossy space, i.e. using a larger time-step size and invariable numerical dispersion errors in any time-step size.

II. FORMULATIONS

For the linear and isotropic plasma, the relative permittivity can be expressed as

$$\varepsilon_r(\omega) = 1 + \frac{\omega_p^2}{\mathrm{j}\omega\gamma - \omega^2} \tag{1}$$

where γ is the collision frequency of the plasma, ω_p is the natural frequency of the plasma.

For the plasma medium, the Ampere's equation in the time domain becomes

$$\nabla \times \mathbf{H}(t) = \varepsilon_0 \frac{\partial \mathbf{E}(t)}{\partial t} + \sigma \mathbf{E}(t) + \mathbf{J}_p(t) \tag{2}$$

where $\mathbf{J}_p(t)$ is the polarization current density which is introduced as the auxiliary variable. The expression of $\mathbf{J}_p(t)$ can be obtained by using the inverse Fourier transformation to the polarization current density in frequency domain. The expression of the polarization current density in frequency domain is expressed as follows:

$$\mathbf{J}_p(\omega) = \mathrm{j}\omega \frac{\varepsilon_0 \omega_p^2}{\mathrm{j}\omega\gamma - \omega^2} \mathbf{E}(\omega). \tag{3}$$

The relationship between $\mathbf{J}_p(t)$ and $\mathbf{E}(t)$ which is the auxiliary differential equation can be obtained by using the inverse Fourier transformation:

$$\frac{\partial \mathbf{J}_p(t)}{\partial t} = -\gamma \mathbf{J}_p(t) + \varepsilon_0 \omega_p^2 \mathbf{E}(t). \tag{4}$$

Then the resulting Maxwell's curl equations for the plasma problem can be obtained as follows:

$$\frac{\partial H_x}{\partial t} = \frac{1}{\mu_0}\left(\frac{\partial E_y}{\partial z} - \frac{\partial E_z}{\partial y}\right) \tag{5}$$

$$\frac{\partial H_y}{\partial t} = \frac{1}{\mu_0}\left(\frac{\partial E_z}{\partial x} - \frac{\partial E_x}{\partial z}\right) \tag{6}$$

$$\frac{\partial H_z}{\partial t} = \frac{1}{\mu_0}\left(\frac{\partial E_x}{\partial y} - \frac{\partial E_y}{\partial x}\right) \tag{7}$$

$$\frac{\partial E_x}{\partial t} = \frac{1}{\varepsilon_0}\left(\frac{\partial H_z}{\partial y} - \frac{\partial H_y}{\partial z} - \sigma E_x - J_{px}\right) \tag{8}$$

$$\frac{\partial E_y}{\partial t} = \frac{1}{\varepsilon_0}\left(\frac{\partial H_x}{\partial z} - \frac{\partial H_z}{\partial x} - \sigma E_y - J_{py}\right) \tag{9}$$

$$\frac{\partial E_z}{\partial t} = \frac{1}{\varepsilon_0}\left(\frac{\partial H_y}{\partial x} - \frac{\partial H_x}{\partial y} - \sigma E_z - J_{pz}\right) \tag{10}$$

$$\frac{\mathrm{d}J_{px}}{\mathrm{d}t} = -\gamma J_{px} + \varepsilon_0 \omega_p^2 E_x \tag{11}$$

$$\frac{\mathrm{d}J_{py}}{\mathrm{d}t} = -\gamma J_{py} + \varepsilon_0 \omega_p^2 E_y \tag{12}$$

$$\frac{\mathrm{d}J_{pz}}{\mathrm{d}t} = -\gamma J_{pz} + \varepsilon_0 \omega_p^2 E_z. \tag{13}$$

In contrast with the conventional FDTD method, the central finite-difference scheme is now used to approximate the spatial derivative only in the PITD method so as to reduce the resulting Maxwell's curl equations to a set of ODEs as follows:

$$\frac{\mathrm{d}H_x|_{i,j+1/2,k+1/2}}{\mathrm{d}t} = \frac{1}{\mu_0}\left(\frac{E_y|_{i,j+1/2,k+1} - E_y|_{i,j+1/2,k}}{\Delta z} - \frac{E_z|_{i,j+1,k+1/2} - E_z|_{i,j,k+1/2}}{\Delta y}\right) \tag{14}$$

$$\frac{\mathrm{d}H_y\big|_{i+1/2,j,k+1/2}}{\mathrm{d}t} = \frac{1}{\mu_0}\left(\frac{E_z\big|_{i+1,j,k+1/2} - E_z\big|_{i,j,k+1/2}}{\Delta x} - \frac{E_x|_{i+1/2,j,k+1} - E_x|_{i+1/2,j,k}}{\Delta z}\right) \quad (15)$$

$$\frac{\mathrm{d}H_z\big|_{i+1/2,j+1/2,k}}{\mathrm{d}t} = \frac{1}{\mu_0}\left(\frac{E_x\big|_{i+1/2,j+1,k} - E_z\big|_{i+1/2,j,k}}{\Delta y} - \frac{E_y\big|_{i+1,j+1/2,k} - E_y\big|_{i,j+1/2,k}}{\Delta x}\right) \quad (16)$$

$$\frac{\mathrm{d}E_x|_{i+1/2,j,k}}{\mathrm{d}t} = \frac{1}{\varepsilon_0}\left(\frac{H_z|_{i+1/2,j+1/2,k} - H_z|_{i+1/2,j-1/2,k}}{\Delta y} - \frac{H_y\big|_{i+1/2,j,k+1/2} - H_y\big|_{i+1/2,j,k-1/2}}{\Delta z} - \sigma E_x|_{i+1/2,j,k} - J_{px}\big|_{i+1/2,j,k}\right) \quad (17)$$

$$\frac{\mathrm{d}E_y\big|_{i,j+1/2,k}}{\mathrm{d}t} = \frac{1}{\varepsilon_0}\left(\frac{H_x|_{i,j+1/2,k+1/2} - H_x|_{i,j+1/2,k-1/2}}{\Delta z} - \frac{H_z|_{i+1/2,j+1/2,k} - H_z|_{i-1/2,j+1/2,k}}{\Delta x} - \sigma E_y\big|_{i,j+1/2,k} - J_{py}\big|_{i,j+1/2,k}\right) \quad (18)$$

$$\frac{\mathrm{d}E_z|_{i,j,k+1/2}}{\mathrm{d}t} = \frac{1}{\varepsilon_0}\left(\frac{H_y\big|_{i+1/2,j,k+1/2} - H_y\big|_{i-1/2,j,k+1/2}}{\Delta x} - \frac{H_x|_{i,j+1/2,k+1/2} - H_x|_{i,j-1/2,k+1/2}}{\Delta y} - \sigma E_z|_{i,j,k+1/2} - J_{pz}\big|_{i,j,k+1/2}\right) \quad (19)$$

$$\frac{\mathrm{d}J_{px}\big|_{i+1/2,j,k}}{\mathrm{d}t} = -\gamma J_{px}\big|_{i+1/2,j,k} + \varepsilon_0\omega_p^2 E_x\big|_{i+1/2,j,k} \quad (20)$$

$$\frac{\mathrm{d}J_{py}\big|_{i,j+1/2,k}}{\mathrm{d}t} = -\gamma J_{py}\big|_{i,j+1/2,k} + \varepsilon_0\omega_p^2 E_y\big|_{i,j+1/2,k} \quad (21)$$

$$\frac{\mathrm{d}J_{pz}\big|_{i,j,k+1/2}}{\mathrm{d}t} = -\gamma J_{pz}\big|_{i,j,k+1/2} + \varepsilon_0\omega_p^2 E_z\big|_{i,j,k+1/2} \quad (22)$$

The above ODEs can be rewritten as a matrix form

$$\frac{\mathrm{d}\mathbf{X}}{\mathrm{d}t} = \mathbf{M}\mathbf{X} + \mathbf{f}(t) \quad (23)$$

where $\mathbf{X} = \left(H_x, H_y, H_z, E_x, E_y, E_z, J_{px}, J_{py}, J_{pz}\right)^T$ is a one-column vector containing both all of the electromagnetic field components and the auxiliary variables, $\mathbf{M}$ is a coefficient matrix determined by the spatial-step size and the medium parameters, and $\mathbf{f}(t)$ is a column vector introduced by the excitations [33].

According to the theory of ODEs, the analytical solution of the equation (23) can be written as

$$\mathbf{X}(t) = e^{\mathbf{M}t}\mathbf{X}(0) + \int_0^t e^{\mathbf{M}(t-s)}\mathbf{f}(s)\,\mathrm{d}s \quad (24)$$

and the discrete form of the equation (24) is

$$\mathbf{X}_{k+1} = \mathbf{T}\mathbf{X}_k + \mathbf{T}^{k+1}\int_{t_k}^{t_{k+1}} e^{-s\mathbf{M}}\mathbf{f}(s)\,\mathrm{d}s \quad (25)$$

where $X_k = X(k\Delta t)$ and $\mathbf{T} = \exp(\mathbf{M}\Delta t)$ is the exponential matrix which can be calculated by the PI technique [37].

Moreover, the Gauss integration technique is used to approximate the integration in the right-hand side of equation (25). Relying our experiments in this area, two-nodes Gauss integrand is accurate enough to satisfy the computational requirement, and the recurrence formula is given by

$$\begin{aligned}\mathbf{X}_{k+1} = \mathbf{T}\mathbf{X}_k &+ \frac{\Delta t}{2}\exp\left[\left(\frac{\Delta t}{2} + \frac{\Delta t}{2}\sqrt{\frac{1}{3}}\right)\mathbf{M}\right] \\ &\times \mathbf{f}\left(t_k + \frac{\Delta t}{2} - \frac{\Delta t}{2}\sqrt{\frac{1}{3}}\right) \\ &+ \frac{\Delta t}{2}\exp\left[\left(\frac{\Delta t}{2} - \frac{\Delta t}{2}\sqrt{\frac{1}{3}}\right)\mathbf{M}\right] \\ &\times \mathbf{f}\left(t_k + \frac{\Delta t}{2} + \frac{\Delta t}{2}\sqrt{\frac{1}{3}}\right). \end{aligned} \quad (26)$$

III. NUMERICAL RESULTS

In order to verify the performance of the proposed method, four typical plasma examples are simulated in the following subsection. The numerical results are also compared with the analytical solution and the results of the JEC-FDTD, ADE-FDTD, RC-FDTD and PLRC-FDTD methods.

A. INFINITE PLASMA SPACE

As the first example, the electromagnetic wave propagation through the infinite plasma space is simulated. The natural frequency of the plasma is $\omega_p = 2\pi \times 10^7$rad/s. The total number of the computational cells is 1000 with 10-cell thick PML layers at the both ends of the computation space. For the JEC-FDTD method and the ADE-FDTD method, in order to satisfy the CFL condition, the spatial-step size is set to $\Delta = 0.125$m, the time-step size is set to $\Delta t = 0.208$ns and the number of the computational time step is 2500. For the proposed PITD method, we simulate the same problem when the time steps are Δt, $3\Delta t$ and $5\Delta t$, respectively. The normalized incident electromagnetic wave is

$$E = \sin^2\left(2\pi \times 10^7 t\right) \quad (27)$$

Fig. 1 gives the waveform of the incident electromagnetic wave. Fig. 2 compares the simulated values of the electric field at the 550th grid from the proposed PITD method, the JEC-FDTD method and the ADE-FDTD method. As shown in Fig. 2, the results obtained by the proposed PITD method are overlapped with the results of the other two

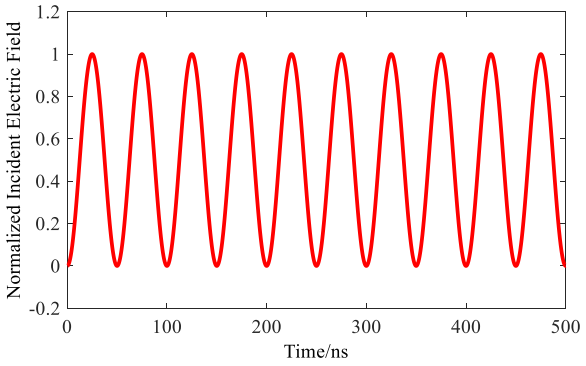

FIGURE 1. The waveform of the incident electromagnetic wave.

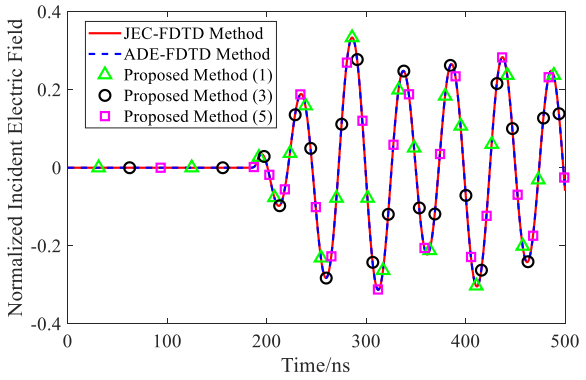

FIGURE 2. The computed values of the electric field at the 550th grid from the JEC-FDTD method, the ADE-FDTD method and the proposed PITD method. Proposed Method (1), Proposed Method (3) and Proposed Method (5) mean the time steps of the proposed PITD method being Δt, $3\Delta t$ and $5\Delta t$, respectively.

FDTD methods in 500ns. Thus, the large time-step size of this method is feasible and effective. Fig. 3 shows the differences of the results by using the proposed PITD method under different time steps from the ADE-FDTD method. It is clearly seen that the differences are nearly independent of the time-step size. Furthermore, the average execution time is 11.85s

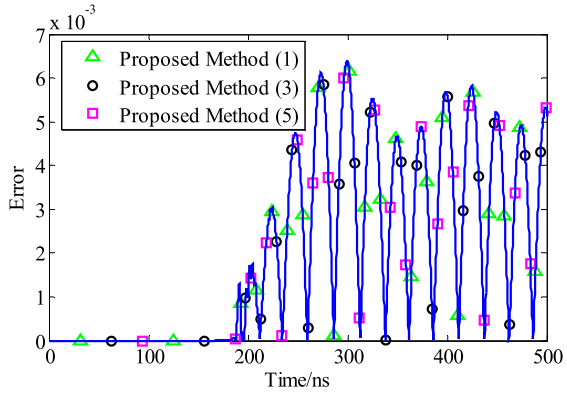

FIGURE 3. The differences of the results by using the proposed PITD method under different time steps from the ADE-FDTD method. Proposed Method (1), Proposed Method (3) and Proposed Method (5) mean the time steps of the proposed PITD method being Δt, $3\Delta t$ and $5\Delta t$, respectively.

for the JEC-FDTD method and 12.45s for the ADE-FDTD method, respectively. When the time-step size is $5\Delta t$, the execution time of the proposed PITD method is 5.93s which is nearly half less than that of the FDTD methods. Therefore, the new method can provide a significant improvement over the JEC-FDTD and ADE-FDTD methods in reducing the simulation times.

B. PLASMA SLAB

To validate the proposed method, the second example is a plasma slab with 1.5cm thick. The computational spatial-step size is set to $\Delta = 75\mu m$. The computational domain consists of 800 grids, with the plasma slab occupying from 300 to 500. In order to reduce the influence of the reflection, 10-cell thick PML layers are set at the both ends of the computational domain. The time-step size of the JEC-FDTD method, ADE-FDTD method, RC-FDTD method and PLRC-FDTD method is $\Delta t = 0.125$ps, and the time-step size of the proposed PITD method is $3\Delta t$. The plasma considered has a plasma frequency of 28.7 GHz ($\omega_p/2\pi$) and a collision frequency γ of 20 GHz.

In order to eliminate the energy of the zero-frequency incident wave, we consider a derivative Gaussian pulse as the incident wave. The spectrum of the derivative Gaussian pulse rises sharply but smoothly from zero frequency, peaks at 50 GHz, and is 10 dB down from this peak at 100 GHz.

Fig. 4(a)-4(c) show the electric field versus cell position after 900-, 1500- and 1900-time steps, respectively. It is clearly seen that the reflection and transmission on the boundary surface and the loss in the plasma slab. Fig. 5 and Fig. 6 show the computational complex reflection coefficients magnitude and phase of the electromagnetic wave propagation through the plasma slab, respectively. Fig. 7 and Fig. 8 show the computational complex transmission coefficients magnitude and phase of the electromagnetic wave propagation through the plasma slab, respectively. It is clearly seen here that the results of the proposed PITD method are very close to those of the JEC-FDTD, ADE-FDTD and PLRC-FDTD method and in agreement with the analytical results quite well. The numerical error of the RC-FDTD method is a little larger than the other methods.

C. PLASMA PHOTONIC CRYSTAL

As the third example, we analyze the band gap characteristics of the plasma photonic crystal. Fig. 9 shows the structure of the plasma photonic crystal. The number of the periodicity is $N = 8$ and $a = b = 1.5$cm. The plasma density is $n = 5 \times 10^{16}\text{m}^{-3}$ and the collision frequency is 3.0GHz. The relative permittivity of the dielectric medium is $\varepsilon_r = 5.0$. The computational spatial-step size is set to $\Delta = 1.5$mm, and the total number of the computational cells is 196 with 10-cell thick PML layers at the both ends of the computation space. The plasma photonic crystal domain is 18 to 178, and the rest is vacuum domain. In order to satisfy the CFL condition, the time-step size of the FDTD method is set to $\Delta t = 2.5$ps and the number of the computational time step

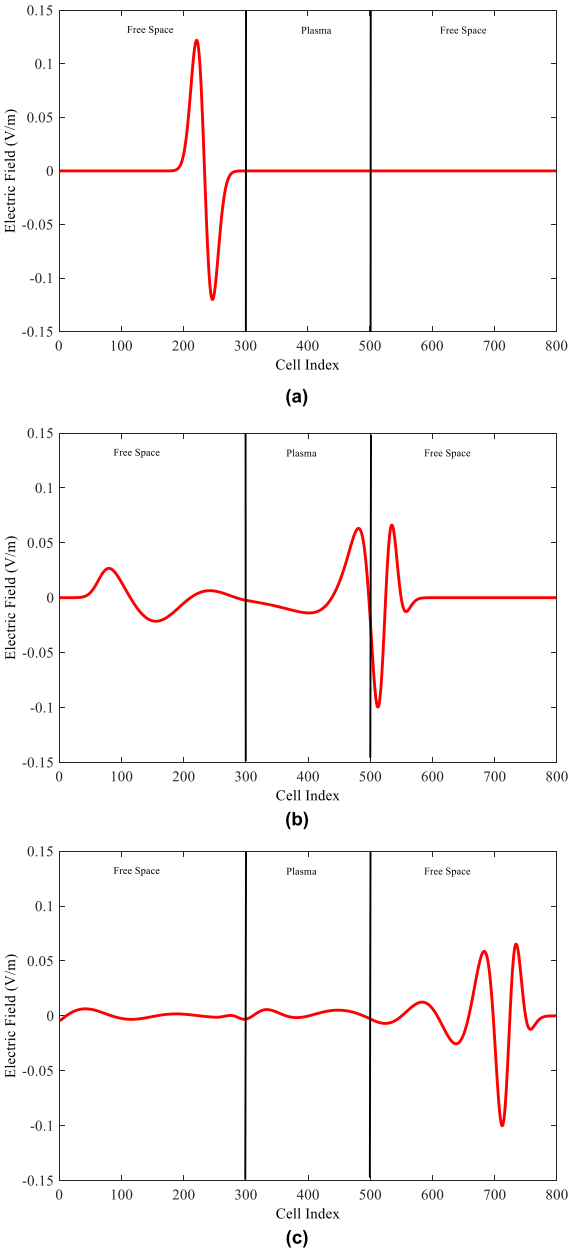

FIGURE 4. The electric field versus cell position after (a) 900-, (b) 1500-, (c) 1900-time steps.

is 50000. For the proposed PITD method, the time-step size is set to $\Delta t = 12.5$ps which is five times the FDTD method.

Fig. 10 and Fig. 11 show the calculated reflection coefficient magnitude and phase of the plasma photonic crystal, respectively. Fig. 12 and Fig. 13 show the calculated transmission coefficient magnitude and phase of the plasma photonic crystal, respectively. According to the reflection spectrum and transmission spectrum, we can observe the band gap characteristics of plasma photonic crystal. The results of the PITD method are also consistent with the FDTD method. Moreover, the execution time of the FDTD method is 8.13s. However, the execution time of the proposed PITD method is just 4.56s.

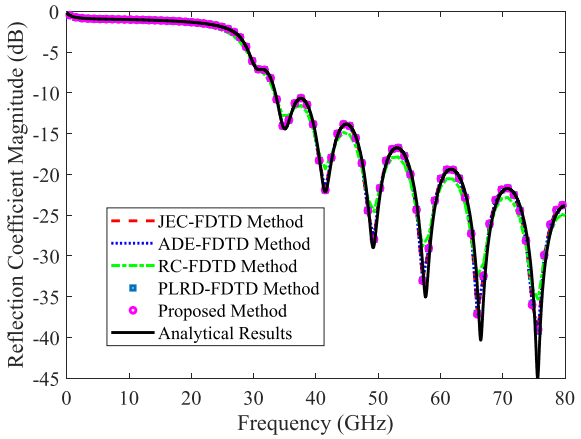

FIGURE 5. The complex reflection coefficient magnitude of the electromagnetic wave propagation through the plasma slab.

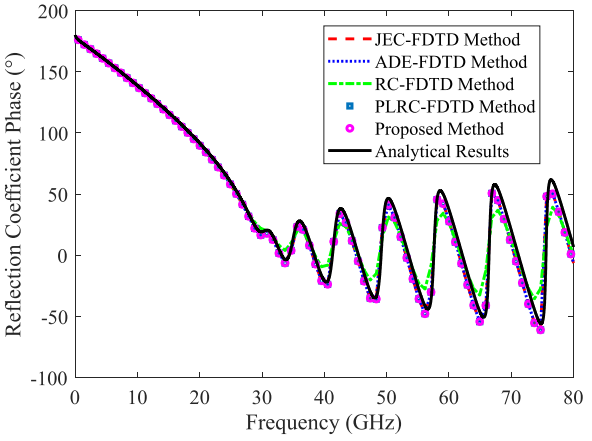

FIGURE 6. The complex reflection coefficient phase of the electromagnetic wave propagation through the plasma slab.

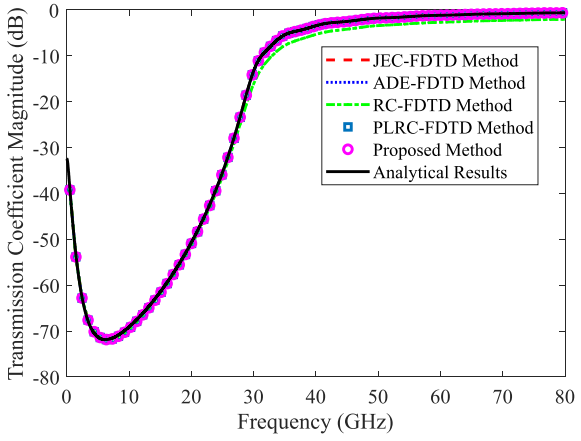

FIGURE 7. The complex transmission coefficient magnitude of the electromagnetic wave propagation through the plasma slab.

D. 2-D PLASMA FILLED CAVITY

The fourth example is a 2-D plasma filled cavity. The mesh of the cavity is 20×20. The spatial-step size is $dx = 75\mu m$. The time-step sizes are 0.1ps for the ADE-FDTD, JEC-FDTD

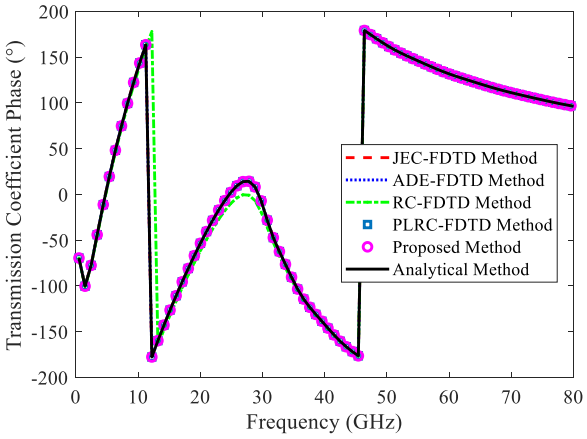

FIGURE 8. The complex transmission coefficient phase of the electromagnetic wave propagation through the plasma slab.

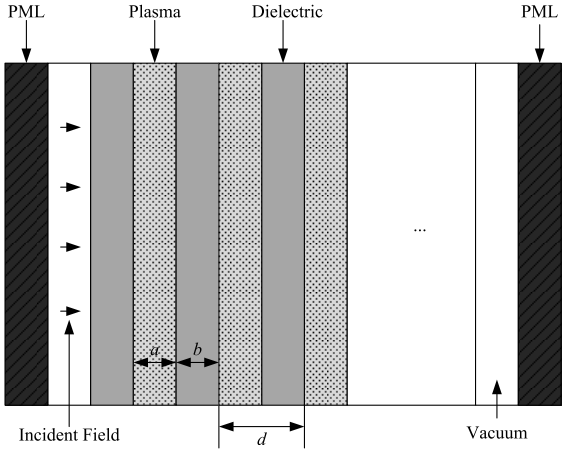

FIGURE 9. The structure of the plasma photonic crystal.

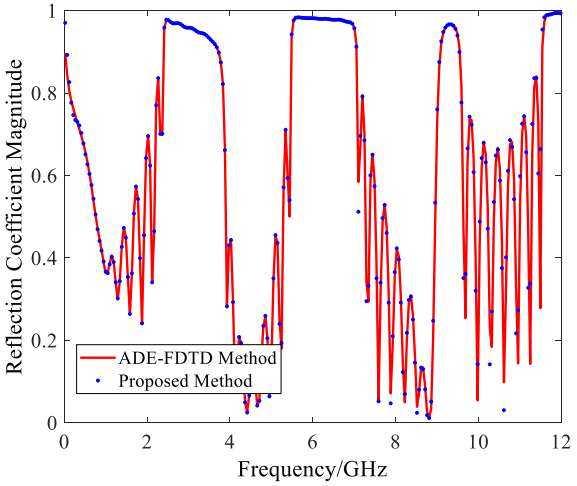

FIGURE 10. The reflection coefficient magnitude of the plasma photonic crystal.

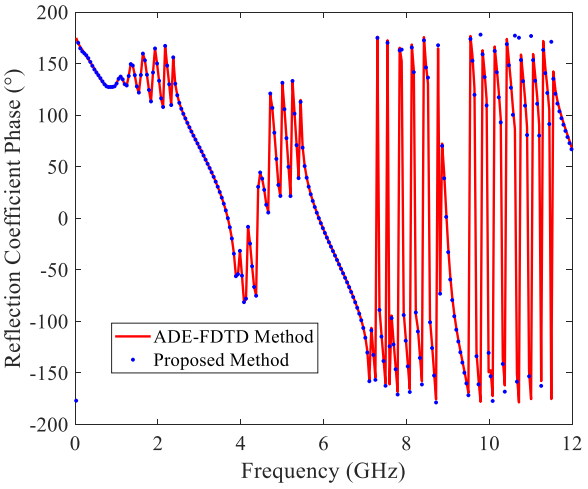

FIGURE 11. The reflection coefficient phase of the plasma photonic crystal.

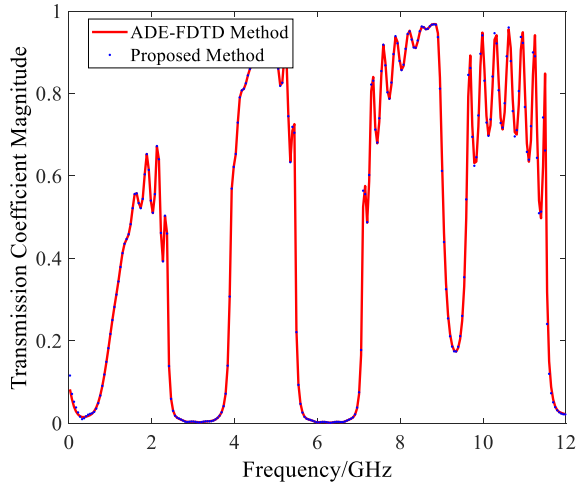

FIGURE 12. The transmission coefficient magnitude of the plasma photonic crystal.

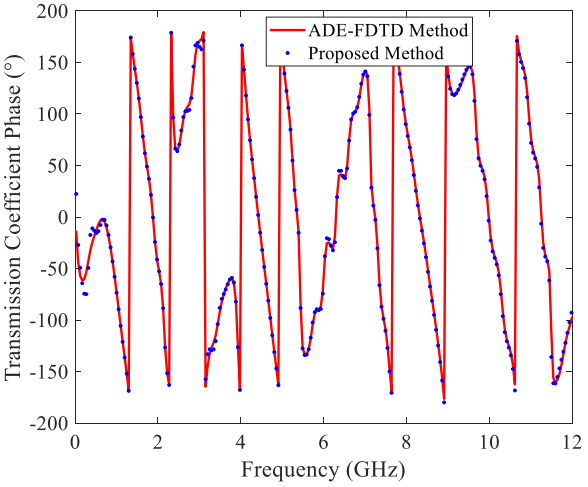

FIGURE 13. The transmission coefficient phase of the plasma photonic crystal.

and PLRC-FDTD methods and 0.6ps for the proposed PITD method, respectively. The parameters of the plasma are same with the second example.

Fig. 14 illustrates the time-domain simulated waveforms of the proposed ADE-PITD method and the other three FDTD methods on the same observation point. We can

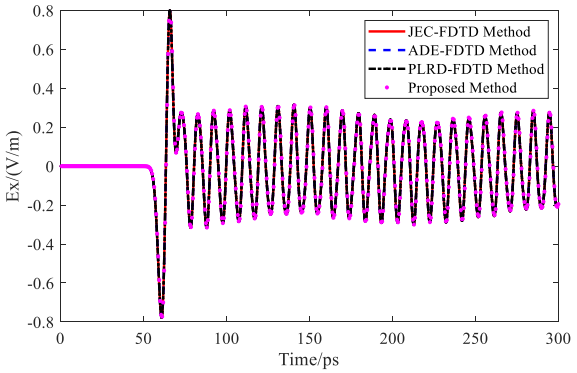

FIGURE 14. The simulated waveform of the 2-D plasma filled cavity.

see that very good agreements are observed between the ADE-PITD method and the other three FDTD methods. In addition, the average execution time of the four methods are: (1) JEC-FDTD method: 6.90s; (2) ADE-FDTD method: 7.15s; (3) PLRC-FDTD method: 6.00s; (4) proposed ADE-PITD method: 4.36s. The average execution time of the ADE-PITD method is about 2/3 of the other methods.

According to the numerical experiments above, it can be concluded that the PITD method is more efficient to solve the plasma problems due to the larger time-step size. The simulations in above analysis are performed on Intel Celeron-M 380 1.60-GHz PC.

IV. STABILITY ANALYSIS

To analyze the stability of the proposed method, the distribution of the eigenvalues of the proposed PITD method is compared with the unit circle. Here, the parameters in example B are used and l is set to 2^{20} in the PITD method. The eigenvalues of the numerical update equations of the proposed PITD method are computed and plotted in the complex plane. According to Von Neumann criterion, if all the eigenvalues of the numerical update equations are less than or equal to unity in magnitude, the recursive scheme is stable.

Fig. 15 shows the distribution of the eigenvalues of the PITD method with respect to the unit circle when the time-step size is changed from Δt to $10^6\Delta t$ (according to the numerical stability condition of the PITD method in free space, the value of the maximum time-step size is about $10^6\Delta t$ when l is set to 2^{20}, Δt is the maximum time-step size allowed by the CFL stability condition in the FDTD method). All the eigenvalues of the PITD method lie within or on the unit circle, i.e., the update equations of the proposed method are stable. Thus, the maximum allowable time-step size of the proposed ADE-PITD method is also much larger than that allowed by the CFL stability condition just like the conventional PITD method.

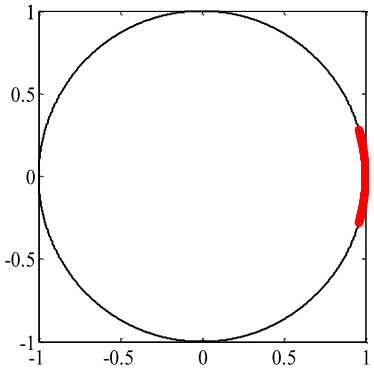

FIGURE 15. Distribution of the eigenvalues in the complex plane for the PITD method when the time-step size is Δt to $10^6\Delta t$.

V. CONCLUSION

In order to break through the CFL stability condition, a modified PITD method for the plasma medium has been proposed with the auxiliary differential equation and the PI technique. Through introducing the polarization current density $\mathbf{J}$ as the auxiliary variable and adding an auxiliary differential equation, the complex permittivity of the plasma is simplified skillfully and the resulting Maxwell's curl equations are obtained. Then approximating the spatial differential derivative with the central finite-difference scheme and applying the PI technique to the temporal operator, we obtain the new formulation which a larger time-step size can be selected. The numerical results have confirmed that this new method is effective for the plasma problem. Furthermore, the numerical results also validate that the selection of the time-step size can break through the limit of the CFL condition and the results are independent of the time-step size. In particular, it is shown that the proposed method is capable of providing the significant improvement over the FDTD methods in reducing the execution times by using a larger time-step size. Thus, this new proposed algorithm is an efficient approach for solving the plasma problems.

REFERENCES

[1] K. S. Yee, "Numerical solution of initial boundary value problems involving Maxwell's equations in isotropic media," *IEEE Trans. Antennas Propag.*, vol. AP-14, no. 3, pp. 302–307, May 1966.

[2] A. Taflove and S. C. Hagness, *Computational Electrodynamics: The Finite-Difference Time-Domain Method*, 3rd ed. Boston, MA, USA: Artech House, 2005.

[3] J. Chen, J. Tan, X. Yu, and H. Shi, "Using WCS-FDTD method to study the plasma frequency selective surface," *IEEE Access*, vol. 7, pp. 152473–152477, 2019.

[4] K. Fujita, "Frequency-dependent MNL-FDTD scheme for wideband analysis of printed circuit boards with debye dispersive media," *IEEE Trans. Antennas Propag.*, vol. 66, no. 10, pp. 5349–5358, Oct. 2018.

[5] X. Ye, M. Y. Koledintseva, M. Li, and J. L. Drewniak, "DC power-bus design using FDTD modeling with dispersive media and surface mount technology components," *IEEE Trans. Electromagn. Compat.*, vol. 43, no. 4, pp. 579–587, Nov. 2001.

[6] J. Chen, J. Li, and Q. H. Liu, "Analyzing graphene-based absorber by using the WCS-FDTD method," *IEEE Trans. Microw. Theory Techn.*, vol. 65, no. 10, pp. 3689–3696, Oct. 2017.

[7] R. Suga, O. Hashimoto, R. K. Pokharel, K. Wada, and S. Watanabe, "Analytical study on change of temperature and absorption characteristics of a single-layer radiowave absorber under irradiation electric power," *IEEE Trans. Electromagn. Compat.*, vol. 47, no. 4, pp. 866–871, Nov. 2005.

[8] K. Fujita, "Dispersive contour-path MNL-FDTD scheme for fast analysis of waveguide metamaterials," *IEEE Trans. Microw. Theory Techn.*, vol. 67, no. 4, pp. 1295–1307, Apr. 2019.

[9] A. Pekmezci and L. Sevgi, "FDTD-based metamaterial (MTM) modeling and simulation [testing ourselves]," *IEEE Antennas Propag. Mag.*, vol. 56, no. 5, pp. 289–303, Oct. 2014.
[10] H. Mosallaei, "FDTD-PLRC technique for modeling of anisotropic-dispersive media and metamaterial devices," *IEEE Trans. Electromagn. Compat.*, vol. 49, no. 3, pp. 649–660, Aug. 2007.
[11] C. L. Holloway, P. M. McKenna, R. A. Dalke, R. A. Perala, and C. L. Devor, "Time-domain modeling, characterization, and measurements of anechoic and semi-anechoic electromagnetic test chambers," *IEEE Trans. Electromagn. Compat.*, vol. 44, no. 1, pp. 102–118, Feb. 2002.
[12] R. Luebbers, F. P. Hunsberger, K. S. Kunz, R. B. Standler, and M. Schneider, "A frequency-dependent finite-difference time-domain formulation for dispersive materials," *IEEE Trans. Electromagn. Compat.*, vol. 32, no. 3, pp. 222–227, Aug. 1990.
[13] J.-F. Liu, H. Lv, Y.-C. Zhao, Y. Fang, and X.-L. Xi, "Stochastic PLRC-FDTD method for modeling wave propagation in unmagnetized plasma," *IEEE Antennas Wireless Propag. Lett.*, vol. 17, no. 6, pp. 1024–1028, Jun. 2018.
[14] R. Wang and G. Wang, "PLRC-WCS FDTD method for dispersive media," *IEEE Microw. Wireless Compon. Lett.*, vol. 19, no. 6, pp. 341–343, Jun. 2009.
[15] M. Okoniewaki, M. Mrozowski, and M. A. Stuchly, "Simple treatment of multi-term dispersion in FDTD," *IEEE Microw. Guided Wave Lett.*, vol. 7, no. 5, pp. 121–123, May 1997.
[16] O. Ramadan, "Stability-improved ADE-FDTD implementation of Drude dispersive models," *IEEE Antennas Wireless Propag. Lett.*, vol. 17, no. 5, pp. 877–880, May 2018.
[17] O. Ramadan, "On the equivalence of the stability of the D-E and J-E ADE-FDTD schemes for implementing the modified Lorentz dispersive model," *IEEE Microw. Wireless Compon. Lett.*, vol. 25, no. 7, pp. 487–488, Jul. 2015.
[18] D. M. Sullivan, "Frequency-dependent FDTD methods using Z transforms," *IEEE Trans. Antennas Propag.*, vol. 40, no. 10, pp. 1223–1230, Oct. 1992.
[19] J. Shibayama, R. Takahashi, A. Nomura, J. Yamauchi, and H. Nakano, "Concise frequency-dependent formulation for LOD-FDTD method using Z transforms," *Electron. Lett.*, vol. 44, no. 16, pp. 949–950, Jul. 2008.
[20] J. Li and J. Dai, "Z-transform implementations of the CFS-PML," *IEEE Antennas Wireless Propag. Lett.*, vol. 5, pp. 410–413, 2006.
[21] W. Chen, Z. Huang, L. Yang, and L. Guo, "Study on the Z-FDTD for electromagnetic scattering characteristics of two-dimensional inhomogeneous plasma sheath," in *Proc. IEEE Int. Conf. Comput. Electromagn. (ICCEM)*, Shanghai, China, Mar. 2019, pp. 20–22.
[22] T. Namiki, "3-D ADI-FDTD method-unconditionally stable time-domain algorithm for solving full vector Maxwell's equations," *IEEE Trans. Microw. Theory Techn.*, vol. 48, no. 10, pp. 1743–1748, Oct. 2000.
[23] F. Zheng, Z. Chen, and J. Zhang, "A finite-difference time-domain method without the courant stability conditions," *IEEE Microw. Guided Wave Lett.*, vol. 9, no. 11, pp. 441–443, Nov. 1999.
[24] F. Zhen, Z. Chen, and J. Zhang, "Toward the development of a three-dimensional unconditionally stable finite-difference time-domain method," *IEEE Trans. Microw. Theory Techn.*, vol. 48, no. 9, pp. 1550–1558, Sep. 2000.
[25] S. J. Cooke, M. Botton, T. M. Antonsen, and B. Levush, "A leapfrog formulation of the 3-D ADI-FDTD algorithm," *Int. J. Numer. Modelling, Electron. Netw., Devices Fields*, vol. 22, no. 2, pp. 187–200, Mar. 2009.
[26] J. Chen, G. Hao, and Q.-H. Liu, "Using the ADI-FDTD method to simulate graphene-based FSS at terahertz frequency," *IEEE Trans. Electromagn. Compat.*, vol. 59, no. 4, pp. 1218–1223, Aug. 2017.
[27] K. Kourtzanidis, F. Rogier, and J.-P. Boeuf, "ADI-FDTD modeling of microwave plasma discharges in air towards fully three-dimensional simulations," *Comput. Phys. Commun.*, vol. 195, pp. 49–60, Oct. 2015.
[28] J. Shibayama, M. Muraki, J. Yamauchi, and H. Nakano, "Efficient implicit FDTD algorithm based on locally one-dimensional scheme," *Electron. Lett.*, vol. 41, no. 19, pp. 1046–1047, 2005.
[29] I. Ahmed, E.-K. Chua, E.-P. Li, and Z. Chen, "Development of the three-dimensional unconditionally stable LOD-FDTD method," *IEEE Trans. Antennas Propag.*, vol. 56, no. 11, pp. 3596–3600, Nov. 2008.
[30] T.-L. Liang, W. Shao, X.-K. Wei, and M.-S. Liang, "Hybrid sub-gridding ADE–FDTD method of modeling periodic metallic nanoparticle arrays," *Chin. Phys. B*, vol. 27, no. 10, Oct. 2018, Art. no. 100204.
[31] T. L. Liang, W. Shao, and S. B. Shi, "Complex-envelope ADE-LOD-FDTD for band gap analysis of plasma photonic crystals," *Appl. Comput. Electromagn. Soc. J.*, vol. 33, no. 4, pp. 443–449, Apr. 2018.
[32] T.-L. Liang, W. Shao, S.-B. Shi, and H. Ou, "Analysis of extraordinary optical transmission with periodic metallic gratings using ADE-LOD-FDTD method," *IEEE Photon. J.*, vol. 8, no. 5, Oct. 2016, Art. no. 7804710.
[33] X. K. Ma, X. T. Zhao, and Y. Z. Zhao, "A 3-D precise integration time-domain method without the restraints of the courant-friedrich-levy stability condition for the numerical solution of Maxwell's equations," *IEEE Trans. Microw. Theory Techn.*, vol. 54, no. 7, pp. 3026–3037, Jul. 2006.
[34] Z.-M. Bai, X.-K. Ma, and G. Sun, "A low-dispersion realization of precise integration time-domain method using a fourth-order accurate finite difference scheme," *IEEE Trans. Antennas Propag.*, vol. 59, no. 4, pp. 1311–1320, Apr. 2011.
[35] G. Sun, X. Ma, and Z. Bai, "A low dispersion precise integration time domain method based on wavelet Galerkin scheme," *IEEE Microw. Wireless Compon. Lett.*, vol. 20, no. 12, pp. 651–653, Dec. 2010.
[36] G. Sun, X. Ma, and Z. Bai, "Numerical stability and dispersion analysis of the precise-integration time-domain method in lossy media," *IEEE Trans. Microw. Theory Techn.*, vol. 60, no. 9, pp. 2723–2729, Sep. 2012.
[37] Z. Kang, X. Ma, and X. Zhuansun, "An efficient 2-D compact precise-integration time-domain method for longitudinally invariant waveguiding structures," *IEEE Trans. Microw. Theory Techn.*, vol. 61, no. 7, pp. 2535–2544, Jul. 2013.
[38] Z. Kang, X. Ma, and Q. Liu, "A high-order 2-D CPITD method for electrically large waveguide analysis," *IEEE Microw. Wireless Compon. Lett.*, vol. 26, no. 2, pp. 83–85, Feb. 2016.
[39] W. X. Zhong and F. W. Williams, "A precise time step integration method," *Proc. Inst. Mechan. Eng. C, J. Mechan. Eng. Sci.*, vol. 208, pp. 427–430, Nov. 1994.

ZHEN KANG (Member, IEEE) was born in Shanxi, China, in 1988. He received the B.S. and Ph.D degrees from the School of Electrical Engineering from Xi'an Jiaotong University, in 2010 and 2016, respectively. From December 2016 to June 2017, he was an Engineer with the Jiangsu Electric Power Company, Research Institute, Nanjing, China. Since July 2017, he has been an Assistant Professor with the School of Automation, Northwestern Polytechnical University, Xi'an, China. His research interests are in the areas of developing the efficiency of the precise-integration time-domain method and numerical methods in solving electromagnetic problems.

WEILIN LI (Member, IEEE) received the B.S. and M.S. degrees in electrical engineering from Northwestern Polytechnical University, Xi'an, China, in 2007 and 2009, respectively, and the Ph.D. (Dr.-Ing.) degree in electrical engineering from the E.ON Energy Research Center, Institute for Automation of Complex Power Systems, RWTH Aachen University, Aachen, Germany, in 2013. He is currently with the Department of Electrical Engineering, Northwestern Polytechnical University, as a Full Professor. He has authored or coauthored for more than 50 peer reviewed journal and conference papers. His research interests are integration of renewable generations, protection in medium voltage DC (MVDC) power systems, and power electronic applications in smart grid.

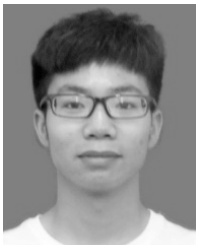

YUFENG WANG received the B.S. degree in electrical engineering from the School of Automation, Northwestern Polytechnical University, Xi'an, China, in 2018, where he is currently pursuing the Ph.D. degree in electrical engineering. His current research interest includes protection in DC power systems.

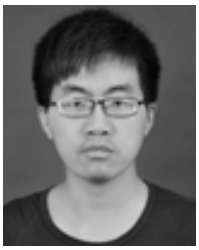

MING HUANG was born in 1989. He received the B.S. degree in electrical engineering from the Hefei University of Technology, Hefei, China, in 2011, and the Ph.D. degree in electrical engineering from Xi'an Jiaotong University, Xi'an, China, in 2019. From October 2017 to October 2018, he was in CURENT, University of Tennessee, Knoxville, as a Visiting Student. His current research interest includes modular multilevel converters in medium-high power applications.

FANG YANG was born in Henan, China, in 1987. She received the B.S. degree from the Henan University of Science and Technology, in 2008, the M.S. degree from the Xi'an University of Science and Technology, Xi'an, China, in 2011, and the Ph.D. degree in electrical engineering from Xi'an Jiaotong University, in 2017. She is currently working with the School of Electrical and Control Engineering with the Xi'an University of Science and Technology. Her current research interests include power electronics and nonlinear dynamics of power electronic converter.